Goodwin, P. M. Allen, D. C. Anderson, E. J. Brown, ibid. 108, 1935 (1989).
8. S. D. Wright and B. C. Meyer, J. Immunol. 136, 1759 (1986).
9. S. K. Lo, P. A. Detmers, S. M. Levin, S. D. Wright, J. Exp. Med. 169, 1779 (1989).
10. T. A. Chatila, R. S. Geha, M. A. Arnaout, J. Cell Biol. 109, 3435 (1989).
11. T. S. Ingebritsen and P. Cohen, Eur. J. Biochem. 132, 255 (1983).
12. C. B. Klee, G. F. Draetta, M. J. Hubbard, Adv. Enzymol. 61, 149 (1987).
13. D. Guerini and C. B. Klee, Proc. Natl. Acad. Sci. U.S.A. 86, 9183 (1989).
14. P. D. Chantler, J. Cell Biol. 101, 207 (1985).
15. M. J. Hubbard and C. B. Klee, Biochemistry 28, 1868 (1989).
16. Y. Hashimoto, B. A. Perrino, T. R. Soderling, J. Biol. Chem. 265, 1924 (1990).
17. The sequence of Cn-412 is ITSFEEAKGLDRINER-MPPRRDAMP, encompassing residues 476 to 501 of subunit A-β of calcineurin and is identical to "peptide 3" in (16). Cn-413 has the sequence GSFPPHRITSFEEAKG (residues 468 to 484). Abbreviations for the amino acid residues are: A, Ala; D, Asp; E, Glu; F, Phe; G, Gly; H, His; I, Ile; K, Lys; L, Leu; M, Met; N, Asn; P, Pro; R, Arg; S, Ser; T, Thr.
18. M. Rechsteiner, Methods Enzymol. 149, 42 (1987).
19. After isolation, neutrophils were allowed to take up by endocytosis a cell-impermeable dye [Lucifer yellow (500 μg/ml) or fluorescein isothiocyanate (FITC)–dextran (50 mg/ml, 70 kD)] or calcineurin inhibitor peptides in incubation buffer for 30 to 40 min at 37°C. The neutrophils were then subjected to a 30-s hypoosmotic shock in water, rinsed in phosphate-buffered saline, and resuspended in incubation buffer. After a minimum of 15 min, motility assays were performed on the cells (Fig. 2). For fluorescence microscopy, the cells were washed three times after exposure to the fluorescent dyes, plated on a glass surface, allowed to spread, and examined on a microscope both before and after an osmotic shock. The cytoplasmic localization of the dye was confirmed by adding trypan blue (200 μg/ml) to quench any residual cell surface fluorescence. In addition, cytoplasmic fluorescence was sensitive to a low concentration of digitonin, a treatment that preferentially permeabilizes the plasma membrane [D. J. Yamashiro, S. R. Fluss, F. R. Maxfield, J. Cell Biol. 97, 929 (1983)]. An assessment of cellular loading was also performed with the use of a homogenization procedure [R. R. Ratan, M. L. Shelanski, F. R. Maxfield, Proc. Natl. Acad. Sci. U.S.A. 83, 5136 (1986)]. The homogenization studies indicated that the cells had taken up 5 ± 4.1% (n = 4) of the external concentration of the dye. In the cytoplasm, the concentration was equal to 4 ± 3.6% of the external concentration of the dye. The amount of dye found in the vesicular fraction ranged from a negligible amount to one-half the amount found in the cytoplasmic fraction. The variability in the compartmentalization of the dye may reflect differences in the effectiveness of osmotic shock or indicate that the homogenization procedure resulted in the artifactual destruction of endosomes and subsequent overestimation of cytoplasmic concentration. A conservative estimate is that the cytoplasmic concentration of the peptide after endocytosis–osmotic shock was 1% of the extracellular concentration of the peptide.
20. J. Liu et al., Cell 66, 807 (1991).
21. _____, Biochemistry 31, 3896 (1992).
22. During the three consecutive 200-s observation periods used in our assay, the number of motile cells was 13 ± 10%, 10 ± 7%, and 14 ± 17% on vitronectin; 55 ± 16%, 30 ± 29%, and 35 ± 22% on fibronectin; and 48 ± 12%, 29 ± 14%, and 27 ± 22% on albumin (mean ± SD).
23. E. G. Hayman, M. D. Pierschbacher, E. J. Ruoslahti, J. Cell Biol. 100, 1948 (1985).
24. P. Cohen, Annu. Rev. Biochem. 58, 453 (1989).
25. _____, C. F. B. Holmes, Y. Tsukitani, Trends Biol. Sci. 15, 98 (1990).
26. H. L. Ostergaard and I. S. Trowbridge, Science 253, 1423 (1991).
27. R. L. Kincaid, M. S. Nightingale, B. M. Martin, Proc. Natl. Acad. Sci. U.S.A. 85, 8983 (1988).
28. M. J. Hubbard and C. B. Klee, in Molecular Neurobiology, J. Chad and H. Wheal, Eds. (IRL Press, Oxford, 1991), p. 135.
29. Incubation with FK506 (100 ng/ml) for a period of 10 min at 37°C was inhibitory; longer incubations at 20°C were required because of the temperature-dependent entry of FK506 into cells. J. J. Siekierka et al., J. Immunology 143, 1580 (1989).
30. We acknowledge J. Poneros for technical assistance and E. Marcantonio for helpful discussions. Funded by NIH grant GM34770 to F.R.M. and NIH research fellowship award GM14150 to B.H.

Diverse Migratory Pathways in the Developing Cerebral Cortex

Nancy A. O'Rourke,* Michael E. Dailey, Stephen J Smith, Susan K. McConnell

During early development of the mammalian cerebral cortex, young neurons migrate outward from the site of their final mitosis in the ventricular zone into the cortical plate, where they form the adult cortex. Time-lapse confocal microscopy was used to observe directly the dynamic behaviors of migrating cells in living slices of developing cortex. The majority of cells migrated along a radial pathway, consistent with the view that cortical neurons migrate along radial glial fibers. A fraction of cells, however, turned within the intermediate zone and migrated orthogonal to the radial fibers. This orthogonal migration may contribute to the tangential dispersion of clonally related cortical neurons.

Newly generated neurons in developing cerebral cortex migrate outward from the ventricular zone, through a cell-sparse intermediate zone, and into the cortical plate below the pial surface of the brain (1). Glial fibers that extend radially from the ventricular to pial surfaces offer a direct pathway for this migration (2, 3). Rakic (4) has proposed that cortical neuronal migration is strictly radial, preserving a point-to-point mapping between the ventricular zone and cortical plate. Lineage studies with retroviral markers, however, indicate that clones derived from single progenitors can have a wide tangential dispersion across the cortex (5, 6). One possible explanation for this result is that the pathways for neuronal migration are more complex than the simple routes offered by radial glia.

To examine directly the migratory behavior and pathways of individual cortical cells, we fluorescently labeled cells in living brain slices and observed their movement using time-lapse confocal microscopy (7). Brain slices allow such imaging studies yet maintain the complex three-dimensional environment in which neurons normally migrate (8, 9). Coronal slices were prepared from neonatal ferret cortex during upper-layer neurogenesis (10) and were maintained in roller tube cultures (11). The following day cells were labeled by focal injection of DiI into the ventricular zone (12), and

N. A. O'Rourke and S. K. McConnell, Department of Biological Sciences, Stanford University, Stanford, CA 94305.
M. E. Dailey and S. J Smith, Department of Molecular and Cellular Physiology, Stanford University School of Medicine, Stanford, CA 94305.

*To whom correspondence should be addressed.

fluorescent cells were imaged in the intermediate zone 12 to 48 hours later (13). Images were obtained 30 to 60 μm below the slice surface to avoid following cells that had migrated beyond the slice onto the cover slip or into the collagen gel. Single optical sections were collected at 1- to 2-min intervals for up to 45 hours, and the pathways and rates of migration were determined.

Visualization of DiI-labeled cells in the intermediate zone revealed cells with bipolar morphologies, elongated cell bodies, thick leading processes, and thinner trailing processes (Fig. 1A). Leading processes extended complex lamellate and filopodial expansions and frequently branched (Figs. 1, 2, and 3). Trailing processes were simpler but also extended filopodia. These morphological features are similar to those of cells in fixed brains presumed to be migrating neurons (2).

Time-lapse sequences revealed the dynamics of migration. Four images of a single cell that exhibited characteristic migratory behavior (Fig. 1) show that both leading and trailing processes rapidly extended and retracted filopodia, behaviors typical of cells exploring their environment (14). The trajectory of the leading process anticipated the direction of movement of the cell soma, although the soma often moved at an independent rate. Here, the leading process advanced rapidly with little cell body movement (Fig. 1, B and C); subsequently, the soma lurched forward (Fig. 1D). The cell body changed shape during this movement, as if squeezing past an obstruction in its environment. The behavior of these cells is reminiscent of that observed in co-cultures of dissociated cerebellar neurons migrating on glia (3).

Among imaged cells, a variety of migratory pathways were traversed. The majority of cells (81.6%; for example, Fig. 1) migrated in a radial or near-radial direction (15) toward the pial surface of the slice. Of 71 cells that moved radially, only one reversed direction to migrate back toward the ventricular zone. The average rate of migration of radially directed cells over the entire imaging period was 11 μm per hour. Cells frequently paused, then resumed movement; thus, the average velocity during movement was higher, roughly 14 μm/hour.

A fraction of cells (12.6%) migrated orthogonal to the radial direction (15) (Fig. 2). One such cell moved initially to the left (Fig. 2A) but switched polarity, converting the trailing into the leading process and reversing direction over the course of 12 min (Fig. 2B). Branches and filopodia extended radially from the leading process (Fig. 2C), as if the cell were exploring (but then ignoring) possible radial routes. On average, orthogonally migrating cells moved faster (30 μm/hour) than radially migrating cells and covered distances up to 350 μm (Fig. 2D). Cells also migrated at angles intermediate between radial and orthogonal: 17.2% of cells were oriented between 30° and 60° from radial (15).

Several cells changed migratory trajectories, making sharp right-angle turns from radial to orthogonal or vice versa. One such cell body initially moved radially but its leading process was bent at a right angle (Fig. 3A). Subsequently, the soma rounded the turn delineated by the leading process (Fig. 3B) and migrated orthogonally. Its leading process then formed branches oriented both radially and orthogonally (Fig. 3C). Right-angle turns were not rare; they were observed in 36.4% of orthogonally and 5.6% of radially migrating cells. Some cells turned at more subtle angles. The cell shown in Fig. 1 migrated initially at an angle about 30° to 40° off radial then made a smooth turn to a radial direction.

To examine whether radial glia were present in cultured slices and thus potentially able to direct migration (3, 4), we fixed and stained slices in whole mount with antibodies to the glial marker vimentin (16). Staining revealed dense palisades of immunoreactive fibers (Fig. 4A) with predominantly radial orientation, terminating in branched endfeet at the pial surface, as do radial glial cells in vivo (17). To assess the relationship between cells observed migrating in time-lapse experiments and radial glia, we fixed slices, photoconverted DiI-labeled migrating cells (18), and immunolabeled the slices for vimentin (Fig. 4). The close apposition between a migrating cell (Fig. 4B) and a vimentin-positive radial process (Fig. 4C) is consistent with the hypothesis that radial migration is supported by radial glial substrates.
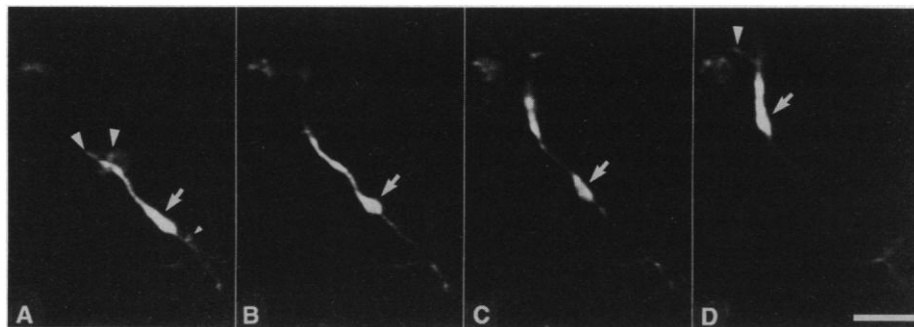

Fig. 1. Time-lapse sequence of a DiI-labeled cell migrating at a near-radial to radial orientation through the intermediate zone of a cortical slice (each panel separated by 55 min). (**A**) A single optical section shows the cell soma (arrow) with a trailing process (small arrowhead) and leading process ending in multiple filopodial extensions (large arrowheads) that extend and retract dynamically. The cell is oriented at a 30° to 40° angle from radial (vertical); the pial surface is up. (**B**) The leading process extended forward, accompanied by a small forward movement of the cell soma (arrow). (**C**) The leading process turned onto a strictly radial orientation, whereas the cell soma (arrow) remained stationary for 1 hour. (**D**) The soma (arrow) translocated forward along the turn defined by the leading process; the leading process itself branched (arrowhead) but showed little forward progress. Scale bar represents 25 μm.
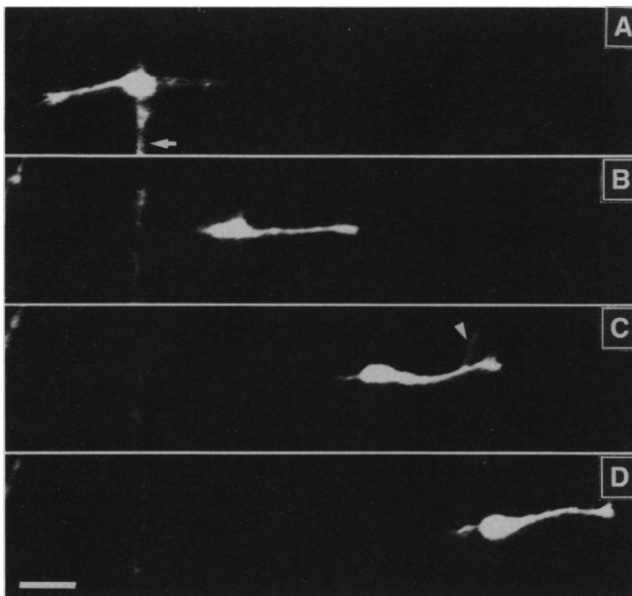

Fig. 2. Time-lapse sequence of a cell migrating orthogonal to the radial direction (each panel separated by approximately 100 min). (**A**) An orthogonally migrating cell moved initially to the left. Radial is delineated by a vertical process (arrow); the pial surface is up. (**B**) The cell reversed its orientation and began to migrate rapidly (24 μm/hour) to the right. (**C**) As the cell migrated, it extended filopodia along radial trajectories (arrowhead). (**D**) The cell withdrew these processes and continued its orthogonal migration for a total of roughly 350 μm. Scale bar represents 25 μm.
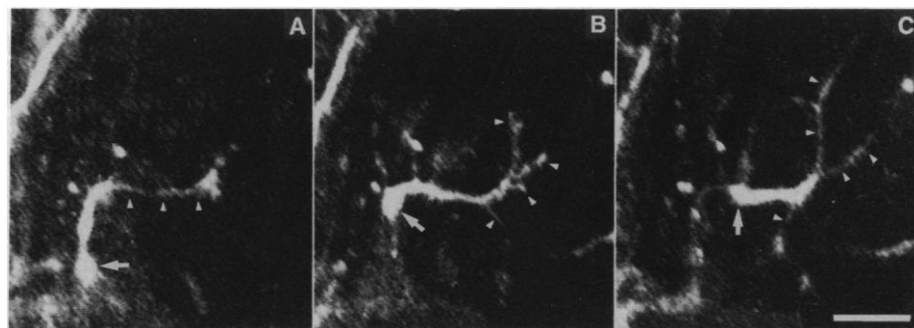

Fig. 3. Time-lapse sequence of cell making a right-angle turn (each panel separated by approximately 2 hours). (**A**) The cell soma (arrow) moved radially while its leading process (arrowheads) was bent in a sharp orthogonal turn. (**B**) The soma (arrow) moved into the turn delineated by the leading process. The leading process formed multiple filopodia (arrowheads), one of which extended radially. (**C**) The cell body (arrow) completed the turn and moved onto an orthogonal trajectory. The filopodia enlarged into several branches (arrowheads), conceivably in anticipation of another turn. Scale bar represents 25 μm.

Fig. 4. (**A**) A single optical section through a slice stained in whole mount with antibodies to vimentin. Palisades of radially oriented glial processes extend through the upper intermediate zone (bottom) into the cortical plate. Branched glial endfeet are seen at the pial surface (top). Migrating cells were imaged only in the intermediate zone, where fibers are largely unbranched. Scale bar represents 50 μm. (**B**) The DiI-labeled cell shown migrating in Fig. 1 was fixed (1 hour after the last panel in Fig. 1 and after further migrating 10 μm radially). The cell was photoconverted into a dark diaminobenzidine reaction product (arrow). (**C**) The same slice was immunostained, and a simultaneous laser scan of the cell shown in (B) was superimposed on a scan of the vimentin staining. A vimentin-positive glial process (arrowheads) is visible adjacent to the migrating cell (arrow). Note the various angles of individual glial fibers; these deviations, all falling within 40° of radial, may account for the near-radial patterns of cell movement. Scale bar represents 10 μm.
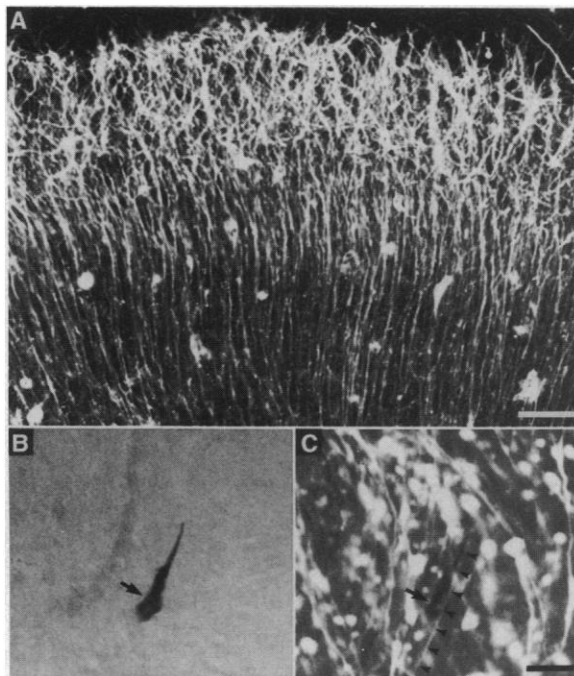
We do not know what substrate supports orthogonal migration. In fixed sections through temporal cortices of retrovirally infected brains, young neurons were observed in postures consistent with orthogonal migration (19). In the temporal cortex, the S-shaped trajectory of radial glia creates a tangentially oriented substrate within the intermediate zone, which suggests that here glial fibers guide even nonradial migration. Our images, however, were obtained from dorsal cortical regions, in which the predominant orientation of glia is radial (Fig. 4A) (17); orthogonally migrating cells were oriented at right angles to the radial fibers. Thus, another cellular substrate may guide orthogonal migration. Cells may migrate along axon tracts extending tangentially through the intermediate zone (20), as implicated in the tangential dispersion of some tectal neurons (21). Orthogonally migrating cells may instead employ extracellular matrix guidance cues. That orthogonal cell movement is roughly three times faster than radial movement suggests that nonglial substrates may underlie orthogonal migration. Alternatively, a subpopulation of rapidly migrating cortical cells may selectively use orthogonal pathways.

We believe that many of the cells we have imaged are fated to become neurons for several reasons. (i) Their morphological features are typical of cells in fixed cortical sections presumed to be migrating neurons (2). (ii) Their dynamic behavior resembles that of migrating cerebellar neurons in vitro (3). (iii) Bromodeoxyuridine studies of mi-

gration in cultured slices demonstrate that postmitotic cells move from the ventricular zone into the cortical plate (8, 9). (iv) These postmitotic cells are normally destined to become upper-layer neurons (10). That lineally related neurons spread tangentially throughout the cortex (5, 6) suggests that neurons that use nonradial migratory pathways can indeed survive and differentiate in the cortical plate.

Here, we have shown directly that the predominant mode of cell migration in the intermediate zone is indeed radial (2–4). However, cells can make sharp right-angle turns onto orthogonal pathways and migrate rapidly for hundreds of microns from their initial radial path. Nonradial migration is likely to occur in intact cortex because orthogonally oriented cells have been noted in the intermediate zone in Golgi-stained sections (22), electron micrographs (23), and in retroviral lineage experiments (6, 19). Thus, orthogonal migration may serve to tangentially disperse neurons that originate at a discrete point within the ventricular zone (24).

REFERENCES AND NOTES

1. J. B. Angevine, Jr., and R. L. Sidman, *Nature* **192**, 766 (1961); P. Rakic, *Science* **183**, 425 (1974); M. B. Luskin and C. J. Shatz, *J. Comp. Neurol.* **242**, 611 (1985).
2. P. Rakic, *Brain Res.* **33**, 471 (1971); *J. Comp. Neurol.* **145**, 61 (1972).
3. J. C. Edmondson and M. E. Hatten, *J. Neurosci.* **7**, 1928 (1987); M. E. Hatten, *Trends Neurosci.* **13**, 179 (1990).
4. P. Rakic, *Science* **241**, 170 (1988).
5. C. Walsh and C. L. Cepko, *ibid.* **255**, 434 (1992).
6. C. P. Austin and C. L. Cepko, *Development* **110**, 713 (1990).
7. M. W. Cooper, A. B. Waxman, S. J. Smith, *Soc. Neurosci. Abstr.* **15**, 808 (1989); S. J. Smith, M. Cooper, A. Waxman, in *Biology of Memory, XXIII Symposium Medicum Hoescht,* L. R. Squire and E. Lindenlaub, Eds. (Schattauer, Stuttgart, 1990), pp. 49–71.
8. J. S. Roberts, N. A. O'Rourke, S. K. McConnell, *Dev. Biol.*, in press.
9. J. Bolz, N. Novak, M. Götz, T. Bonhoeffer, *Nature* **346**, 359 (1990).
10. S. K. McConnell, *J. Neurosci.* **8**, 945 (1988); C. A. Jackson, J. D. Peduzzi, T. L. Hickey, *ibid.* **9**, 1242 (1989).
11. Brain slices were prepared for culture as modified (8) from B. H. Gähwiler [*J. Neurosci. Methods* **4**, 329 (1981)]. Postnatal day 0 (P0) to P1 ferret kits (Marshall Farms, North Rose, NY) were killed by decapitation, in accordance with institutional guidelines. Brains were cut into 400-μm coronal slices [L. C. Katz, *J. Neurosci.* **7**, 1223 (1987)], embedded in Vitrogen (CellTrix, Santa Clara, CA), and cultured in a roller drum (8).
12. After 24 hours in culture, cells were labeled with the fluorescent lipophilic dye DiI [DiIC$_{18}$(3), Molecular Probes, Eugene, OR] [M. G. Honig and R. I. Hume, *J. Cell Biol.* **103**, 171 (1986)]. Pressure injections of DiI (0.1 to 0.2 nl, 0.5% in dimethyl formamide) were made through a micropipette into the ventricular zone, labeling small areas (~50 to 100 μm diameter). Slices were returned to the roller drum for 12 to 48 hours to allow dye incorporation and cell migration away from injection sites. Slices were imaged after 2 to 3 days in culture, before slices thinned appreciably.
13. Migrating cells in the intermediate zone were visualized with the use of time-lapse imaging with two laser-scanning confocal microscopes (one made by S. J Smith, one a modified Bio-Rad MRC-500 with Zeiss IM-35). Slices were warmed to 32° to 35°C and viewed with the use of a ×20 Fluor (Nikon), ×25 Plan-Neofluor oil (Zeiss), or ×40 DApo UV (Olympus) objective. Images of a single focal plane were collected with single laser scans every 1 or 2 min and stored with the use of an analog recorder (OMDR, Panasonic, Secaucus, NJ). Images were played back to assess cell movement. If no movement was detected after 20 to 30 min, the slice was discarded; approximately 25% of slices displayed migration. Slices with migrating cells (*n* = 87 cells from 19 slices) were observed for up to 45 hours (average is 8.2 hours).
14. S. J Smith, *Science* **242**, 708 (1988).
15. The radial direction was estimated from sketches of the laser-scanned area on drawings of each slice and from the orientation of fibers (the majority of which were radial) in each field. For quantitative analysis, we define radial and near-radial as vectors of movement that fall within 30° of the radial direction and orthogonal as those falling within 70° to 100° of radial. The total percentage of cells cited in the text is greater than 100% because 10 cells turned, thus migrating in two directions.
16. Slices were fixed in 4% paraformaldehyde, rinsed [phosphate-buffered saline (PBS), 30 min], and extracted (1% Triton X-100 in PBS for 1 to 2 days at room temperature). Radial glia were visualized with mouse monoclonal antibodies against vimentin [Boehringer Mannheim; 1:10 in PBS with bovine serum albumin (100 mg/ml) and 1% Triton] followed by biotinylated secondary antibodies and fluorescein-Avidin D (Vector).
17. T. Voigt, *J. Comp. Neurol.* **289**, 74 (1989); D. E. Schmechel and P. Rakic, *Anat. Embryol.* **156**, 115 (1979); J. F. Gadisseux, P. Evrard, J. P. Misson, V. S. Caviness, *Dev. Brain Res.* **50**, 55 (1989).
18. S. K. McConnell, A. Ghosh, C. J. Shatz, *Science* **245**, 978 (1989); J. H. Sandell and R. H. Masland, *J. Histochem. Cytochem.* **36**, 555 (1988).
19. J.-P. Misson, C. P. Austin, T. Takahashi, C. L. Cepko, V. S. Caviness, *Cereb. Cortex* **1**, 221 (1991).
20. Boulder Committee, *Anat. Rec.* **166**, 257 (1970).

21. G. E. Gray and J. R. Sanes, *Neuron* 6, 211 (1991).
22. L. J. Stensaas, *J. Comp. Neurol.* 131, 409 (1967); *ibid.*, p. 423; D. K. Morest, *Z. Anat. Entwicklungsgesch.* 130, 265 (1970).
23. G. M. Shoukimas and J. W. Hinds, *J. Comp. Neurol.* 179, 795 (1978).
24. Walsh and Cepko (5) estimated that ~40% of retrovirally tagged clones disperse tangentially in rat cortex, whereas 12.6% of imaged ferret cells migrated orthogonally. Whether orthogonal migration in the intermediate zone could account completely for the dispersion of cortical clones remains unclear for several reasons. (i) Tangential migration may also occur in other regions, such as the ventricular zone [G. Fishell, C. A. Mason, M. E. Hatten, *Soc. Neurosci. Abstr.* 18, 926 (1992)] or cortical plate. (ii) The extent of orthogonal migration may differ in rats. (iii) We have examined coronal slices; orthogonal migration may occur in other planes as well. (iv) Quantitative aspects of orthogonal migration may be altered if preferred paths are cut by sectioning or diffusible signals are impaired in cultured slices.
25. We thank T. Schwarz and C. Shatz for comments on the manuscript, J. Roberts for advice on culturing brain slices, and C. Kaznowski for help with photography. Supported by grants from NIH (EY06314 to N.A.O'R., NS09027 to M.E.D., and NS28587 to S.JS.), the National Institute of Mental Health (Silvio Conte Center for Neuroscience Research, MH48108), and from Searle Scholars, Pew Scholars, NSF Presidential Young Investigator, and a Clare Boothe Luce Professorship to S.K.M.

Prevention of Programmed Cell Death of Sympathetic Neurons by the *bcl-2* Proto-Oncogene

Irène Garcia, Isabelle Martinou, Yoshihide Tsujimoto,* Jean-Claude Martinou†

Approximately half of the neurons produced during embryogenesis normally die before adulthood. Although target-derived neurotrophic factors are known to be major determinants of programmed cell death—apoptosis—the molecular mechanisms by which trophic factors interfere with cell death regulation are largely unknown. Overexpression of the *bcl-2* proto-oncogene in cultured sympathetic neurons has now been shown to prevent apoptosis normally induced by deprivation of nerve growth factor. This finding, together with the previous demonstration of *bcl-2* expression in the nervous system, suggests that the Bcl-2 protein may be a major mediator of the effects of neurotrophic factors on neuronal survival.

Programmed cell death—apoptosis—is an active process of self-destruction that occurs in normal vertebrate development (1). Although RNA and protein synthesis seem to be required for many cells to die (2), the molecular pathways that regulate programmed cell death are unknown. Evidence suggests that, in neurons, this process is initiated under conditions in which the concentration of target-derived neurotrophic factors is reduced (3). The *bcl-2* proto-oncogene product (4) delays the onset of apoptotic cell death in B cells (5) and in T cells (6), and we now show that *bcl-2* overexpression prevents neuronal death induced by trophic factor deprivation.

In the presence of nerve growth factor (NGF), sympathetic neurons can be maintained in culture for several weeks; NGF deprivation induces neuronal death by an apoptosis-like mechanism that requires

both mRNA and protein synthesis (7) and which is accompanied by nuclear DNA fragmentation (8). To assess the effect of *bcl-2* on neuronal death, we constructed the expression vector EB-2, consisting of 1.8 kb of 5' flanking DNA of the rat neuron-specific enolase promoter linked to a DNA fragment encoding human *bcl-2* (9), and microinjected this construct into the nucleus of cultured rat sympathetic neurons (Fig. 1A). Approximately 80 to 90% of injected neurons survived the stress caused by the injection; damaged cells died less than 3 hours after injection and were not included in the results.

The percentage of injected neurons that expressed *bcl-2* was determined in cultures of neurons growing in an NGF-rich medium by means of a species-specific monoclonal antibody to human Bcl-2 (10). Twenty-four hours after injection, approximately 80% of the neurons that received a solution containing DNA reacted with anti–Bcl-2. [Co-injection of DNA with fluorescein isothiocyanate (FITC)–conjugated dextran in some cells demonstrated the efficacy of the injection procedure (Fig. 1, B and C).] This percentage decreased to $43 \pm 2\%$ (mean $\pm$ SEM, $n = 4$) (Fig. 1D) 3 days after injection and to 10% by day 10.

In lymphocytes, the Bcl-2 protein has

been localized to the inner mitochondrial membrane (11). Observation of neurons expressing *bcl-2* with a confocal microscope revealed a punctate cytoplasmic immunostaining (Fig. 1E), resembling that of rhodamine 123, which specifically targets mitochondria (12) (Fig. 1F). This observation suggests that the protein is targeted to mitochondria in both neurons and lymphocytes. However, we cannot exclude another subcellular localization of Bcl-2 in neurons.

The effects of *bcl-2* on neuronal survival were investigated in low-density cultures (500 neurons per square centimeter) in which cells are prevented from clustering in small groups, thus facilitating cell injection as well as cell counting. Non-neuronal cells, a possible source of NGF, were virtually eliminated by the presence of 10 μM cytosine arabinoside C in the culture medium. Experiments were performed on 7-day-old cultures because the NGF dependency of sympathetic neurons in vitro has been shown to decrease with time in culture (7, 13). NGF-containing medium was replaced with NGF-free medium 3 hours after injection. In some experiments, antibodies to NGF were added to the NGF-free medium to accelerate neuronal degeneration.

In control conditions (no injection or injection with control pNSE-LacZ vector), neuronal death—phase-dark cell body and neurite disintegration—was first apparent within 48 hours after NGF deprivation. By 72 hours, only 10% of the initial neuronal population had survived (Fig. 2E); these neurons may have survived because of nearby remaining non-neuronal cells. A more marked degeneration was observed in the presence of anti-NGF. At 72 hours, almost all neuronal cells had disappeared (Fig. 2, A and E). In contrast, 40 to 50% of the initial neuronal population injected with EB-2 (depending on the absence or presence of anti-NGF (Fig. 2E) displayed phase-bright cell bodies with thick neurites that adhered to the collagen substratum (Fig. 2B). The viability of these neurons was confirmed by staining with the vital marker acridine orange (14) (Fig. 2C). They also reacted with anti–Bcl-2 (Fig. 2D). EB-2–injected neurons were capable of surviving for more than 1 week in the absence of NGF (Fig. 2F). By day 10, the number of surviving neurons decreased to about 20%, possibly because of reduced synthesis of Bcl-2 with time. There was a clear correlation between the percentage of neurons containing Bcl-2 (in terms of efficacy and duration of transfection) and the percentage of neurons protected from death, suggesting that every neuron expressing *bcl-2* was capable of surviving in the absence of NGF. At day 12, the rescued

I. Garcia, Department of Pathology, Centre Médical Universitaire, 1211 Geneva 4, Switzerland.
I. Martinou and J.-C. Martinou, Department of Pharmacology and Clinical Neurophysiology, Centre Médical Universitaire, 1211 Geneva 4, Switzerland.
Y. Tsujimoto, Wistar Institute, Philadelphia, PA 19104–4268.

*Present address: Osaka University Medical School, Biomedical Research Center, Suita, Osaka 565, Japan.
†To whom correspondence should be addressed.